Effect of Network Structure and Committed Minority Placement in Promoting Social Diffusion

Effect of network structure and committed minority placement in promoting social diffusion

Tianshu Gao, Lorenzo Zino, *Member, IEEE,* Mengbin Ye, *Member, IEEE,*

***Abstract*—Social diffusion is the phenomenon whereby a population collectively adopts a novel (alternative) behaviour, opinion, product or technology to replace an existing status quo. Often the process is driven by a small number of individuals, termed committed minority, who stubbornly promote the alternative. In this work, we use an experimentally-proven game-theoretic agent-based model to explore how social diffusion is influenced by the network of social interactions, the placement of committed minority and the timing that committed minority are introduced into the network. Through a campaign of Monte Carlo simulations, we find that diffusion occurs quicker on sparse and highly-clustered networks. In addition, we show that placing the committed minority at nodes with the highest Bonacich centrality with a negative attenuation factor seems to be the best approach for facilitating diffusion. Then, we find that the timing of introducing committed minority has a negligible effect on the diffusion process. Finally, our findings are tested and confirmed on two case studies of real-world networks.**

***Index Terms*—Social diffusion; centrality measures; social networks; agent-based**

I. Introduction

A. Background on Social Diffusion

SOCIAL diffusion refers to the collective adoption of a new *alternative* behaviour, opinion, product, or technology by a population to replace a *status quo*, in a process that is primarily driven by interactions among the population rather than by regulations or policies [1]–[5]. In many instances, these interactions involve social influence and coordination, whereby individuals benefit from coordinating on the same choice [6]. There is a strong interest in the scientific community to develop theories and models of social diffusion, as this phenomenon has relevance in many different application domains, including adoption of medical preventive interventions [7], [8], new cultural traits [2], emergency response [9], and environmentally-friendly practices [10].

Besides social influence and coordination, there could be many other driving forces that can help promote social diffusion. Recently, two of them have received particular interest in the social diffusion literature. The first is *choice advantage*, that is, when the alternative gives more benefits to individuals than the status quo. Successful diffusion of the alternative has been linked to a sufficiently large advantage [4], [5], [11]. The second is the presence of *committed minority* (also termed as committed individuals) who stubbornly choose the alternative instead of the status quo. Since interactions underpin social diffusion, the presence of a sufficiently large committed minority, who interact with uncommitted individuals, can also lead to successful diffusion [1], [12].

Social diffusion can be studied empirically, using field data and/or sociological experiments [1], [2], [12]–[15]. These studies have explored a wide range of issues, including the aforementioned factors of choice advantage and committed minority. One of the robust findings of empirical and experimental studies is the 'S-shaped' adoption curve, which describes the fraction of alternative adopters over time [16], [17]. Besides field studies and experiments, mathematical models of diffusion have also emerged as viable approaches to studying the phenomenon of social diffusion.

B. Literature Review of Models of Social Diffusion

Here, we provide a brief review of the state-of-the-art literature in mathematical modelling of social diffusion. We focus on agent-based models, which in the past two decades have become especially popular for studying social diffusion thanks to their ability to simulate the actions and interactions of agents (individuals) in a large population over time [18]. One of the key advantages of ABMs is that they are able to link individual-level (microscopic level) dynamics to the emergence of population-level (macroscopic level) phenomena [19], thereby allowing researchers to explore how individual- and group-level factors can affect the social diffusion process. For instance, ABMs have been used to study the impact of limited individuals' rationality [4], [5], [20], population heterogeneity [1], [21], constraints on the interactions among agents, external interventions [22] and positive externalities [23].

One class of ABMs that has been traditionally used to study social diffusion are epidemic models, originally developed to study the spread of infectious diseases. The underlying assumption of such models is that the probability an individual adopts the alternative increases for each interaction they have with another individual who has already adopted the alternative [24]–[27]. The key conclusions drawn from such models include: (*i*) Diffusion occurs quickly in highly connected networks; (*ii*) Clusters in a network hamper diffusion while long-range connections accelerate it; (*iii*) Nodes with high degree are key for social diffusion. However, epidemic models fail to capture the complex interaction patterns that can arise during social diffusion [28], and this may lead to erroneous conclusions, as noted in [20].

T. Gao and M. Ye are with the Centre for Optimisation and Decision Science, Curtin University, Bentley 6102, WA, Australia. Emails: tianshu.gao1@postgrad.curtin.edu.au, mengbin.ye@curtin.edu.au. L. Zino is with the Department of Electronics and Telecommunications, Politecnico di Torino, Torino, Italy. Email: lorenzo.zino@polito.it. M. Ye is supported by the Western Australian Government through a Defence Science Centre Collaborative Research Grant and by the Premier's Science Fellowship Program.

To address these limitations, game-theoretic models have become increasingly popular in the study of social diffusion over the past two decades. These models assume that individuals can repeatedly revise their decisions on the choice between the status quo and the alternative over time, and each individual's decision can influence other individuals' decisions. Decisions are made in a game-theoretic framework: each individual obtains a payoff from selecting the status quo and the alternative, and individuals tend to base their choice on maximising their payoff. Since individuals tend to coordinate on their choice, these models are typically based on games involving coordination. In [29], Kandori *et al.* studied a coordination game-theoretic model and proved convergence to an equilibrium in which all agents adopt the same choice. This work was mainly focusing on the scenario in which each agent knows every other agents' choices, i.e. interaction network is fully connected. In [30], Ellison *et al.* explored the impact of restricting agents to local interactions. This line of research has been further developed in [20], where the convergence rate is estimated as a function of the network structure on which individuals can interact. A key conclusions is that, unlike what was observed with epidemic models, high-degree nodes and long-range connections slow down the diffusion process.

Using game-theoretic ABMs, many works have studied choice advantage as the driving force of social diffusion [4], [20], [29], [30]. In contrast, there have been few game-theoretic ABMs that focus on committed individuals as the main driver of diffusion. Both choice advantage and committed minority were examined in [11], while the number of the committed individuals needed to guarantee diffusion was studied in [1]. Importantly, a series of group experiments was conducted in [1]; the experimental data led to the proposal of a game-theoretic model that, besides coordination, included two additional mechanisms of inertia and trend-seeking, well known in the social-psychology literature [31], [32]. The experimental data was also used to identify the ABM parameters.

C. Main Contribution of This Paper

In this paper, we extend this effort. Specifically, [1] was focused on understanding how many committed minority were needed to guarantee social diffusion in a fully-connected population, while the important role of the network of social interactions were neglected. Here, we use the experimentally-grounded ABM developed and calibrated in [1] to investigate several important research questions related to the complexity of real-world networks of social interactions and concerning the possibility to design effective strategies to place the committed minority to unlock social diffusion. Using committed minority as the driving force for social diffusion, our investigations yield the following key contributions.

First, we explore how the network structure influences social diffusion, including the speed of diffusion and the likelihood that diffusion occurs. By performing a campaign of Monte Carlo numerical simulations over different classes of networks with different features in terms of sparsity and clustering, we find that highly connected networks hamper social diffusion. This contradicts the conclusions obtained using epidemic models, but is consistent with the findings of game-theoretic models [20]. In addition, we find that clustering affects the diffusion process. In particular, we observe that diffusion is more likely to occur in highly-clustered networks, similar to what observed in other game-theoretic models [20], but we additionally show that it typically takes more time. This finding provides more nuance to our understandings of the role of clustering in social diffusion.

Second, we explore the possibility to locate committed individuals in the network in a suitable way to accelerate the social diffusion process. To this aim, we test different placement schemes, based on different network centrality measures [33]. Our numerical findings suggest that Bonacich centrality with a negative attenuation factor is the best way to position the committed minority. This finding reveals that nodes who are connected to isolated nodes are the gateway for successful diffusion. In other words, it is not the degree of a node, but rather how many low-degree nodes a node is connected to, that determines the importance of the node. This insightful finding opens new directions for determining critical actors in social diffusion processes.

Third, since emerging trends were found to play an important role in the diffusion process [1], [11], [32], we test whether introducing the committed individuals gradually over a period of time to create a (manufactured) trend towards the alternative may be beneficial to facilitate social diffusion. Our findings suggest that trivial implementations of gradual introductions of the committed individuals over time have an insignificant impact on the social diffusion process, suggesting that future effort should be placed toward investigating more refined strategies.

Fourth, in order to solidify our findings, we investigate two case studies of real-world social networks of sizes and with different characteristics, in which we test our ABM and the insights derived regarding network topology and committed minority placement on a real-world network structure [34]. The analysis of the case studies supported our findings, highlighting the key role of sparsity and clustering in facilitating social diffusion, and confirming the effectiveness of locating the committed minority in nodes with high Bonacich centrality with a negative attenuation factor.

In summary, our main contributions, supported by the analysis of different classes of synthetic networks and the two real-world case studies, are the following:

- We show that sparse and highly-clustered networks increase the likelihood of social diffusion, although the latter may result in slower diffusion.
- We discover that the positioning of committed minority on the network can be key to achieving social diffusion. In particular, targeting nodes with high Bonacich centrality with negative attenuation factor proves highly effective across all types of networks.
- We find that trivial implementations of gradual introductions of the committed individuals over time have a negligible impact on social diffusion.

The rest of paper is structured as follows. In Section II, we present mathematical preliminaries and the diffusion model, and formulate the research questions. Then, our main results

are presented in Sections III, IV and V. In Section VI, we discuss the two case studies. Section VII concludes the paper.

II. Preliminaries and Problem Formulation

In this section, we first review elements of graph theory and then describe the decision-making model used to study social diffusion. After that, we introduce four classes of networks and different centrality approaches that will be used in our study. Last, we formulate our research questions.

A. Graph Theory

An undirected unweighted graph is a tuple $\mathcal{G} = (\mathcal{V}, \mathcal{E}, \boldsymbol{A})$, where $\mathcal{V} = \{1, \ldots, n\}$ is the set of $n \geq 2$ nodes, $\mathcal{E} \subseteq \mathcal{V} \times \mathcal{V}$ is the set of (undirected) edges, and $\boldsymbol{A} \in \mathbb{R}^{n \times n}$ is the adjacency matrix. The element $e_{ij} = (i, j) \in \mathcal{E}$ denotes an undirected edge between nodes i and j (because the edge is undirected, e_{ij} can also be written as e_{ji}). Self-loops are not permitted, i.e. $e_{ii} \notin \mathcal{E}$, for all $i \in \mathcal{V}$. The adjacency matrix $\boldsymbol{A} = \{a_{ij}\}$ has entries $a_{ij} = a_{ji} = 1$ if and only if $(i, j) \in \mathcal{E}$, and $a_{ij} = a_{ji} = 0$ otherwise. Node i and node j are said to be neighbours if $(i, j) \in \mathcal{E}$. The set of neighbours of i is given by $\mathcal{N}_i = \{j \in \mathcal{V} : (i, j) \in \mathcal{E}\}$. The degree of node i, denoted by $d_i = \sum_{j=1}^{n} a_{ij}$ is the number of neighbours of i. The average degree of the graph is denoted by $d = \sum_{i=1}^{n} d_i / n$. A path between node i_1 and node i_k is a sequence of distinct edges of the form $(i_1, i_2), (i_2, i_3), \cdots, (i_{(k-1)}, i_k)$, where $i_j \in \mathcal{V}$ and $(i_j, i_l) \in \mathcal{E}$. The length of a path is equal to the number of edges in the path, and the geodesic distance between two nodes i and j, denoted as ℓ_{ij}, is the length of the shortest path between these two nodes. A graph is connected if there exists a path between every pair of nodes.

B. Game-Theoretic Decision-Making Model

We consider a population $\mathcal{V} = \{1, \cdots, n\}$ of $n \geq 2$ individuals, interacting on a connected network $\mathcal{G} = (\mathcal{V}, \mathcal{E}, \boldsymbol{A})$. At each time-step $t = 1, 2, ...$, individuals are able to revise their choices from a binary strategy set $\mathcal{S} = \{0, 1\}$, where 0 represents the status-quo and 1 represents the alternative. The strategy choice of individual $v \in \mathcal{V}$ at time-step t is denoted by $x_v(t) \in \mathcal{S}$. At each time-step, each individual may revise their strategy according to a noisy myopic best-response (loglinear learning). Namely, the probability of individual v choosing strategy $x \in \mathcal{S}$ at the next time-step is given by

$$\mathbb{P}[x_v(t+1) = x] = \frac{\exp\{\beta_v \pi_v(x)\}}{\exp\{\beta_v \pi_v(0)\} + \exp\{\beta_v \pi_v(1)\}}, \quad (1)$$

where $\beta_v \in [0, \infty)$ denotes the rationality of individual v and $\pi_v(x)$ denotes the payoff for individual v choosing strategy $x \in \mathcal{S}$, which is detailed below. We say that β_v captures the bounded rationality of individual v because $\beta_v = 0$ means that both strategies have a uniform probability to be chosen, while as $\beta_v \to \infty$, the probability that individual v chooses the strategy that has a higher payoff approaches 1.

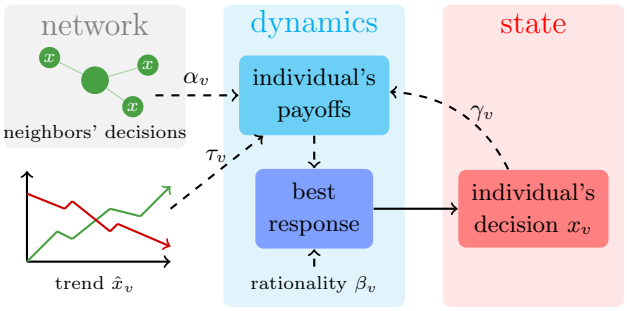

Fig. 1. Flow chart of the operating mechanism of the Game-Theoretical Decision-Making Model

The payoff $\pi_v(x)$ is defined as

$$\pi_v(1) = \frac{\alpha_v}{d_v} \sum_{w \in \mathcal{N}_v} x_w(t) + \gamma_v x_v(t) + \tau_v \hat{x}_v(t), \quad (2a)$$

$$\pi_v(0) = \frac{\alpha_v}{d_v} \sum_{w \in \mathcal{N}_v} (1 - x_w(t)) + \gamma_v (1 - x_v(t)) + \tau_v (1 - \hat{x}_v(t)), \quad (2b)$$

with

$$\hat{x}_v(t) = \frac{1}{2}\Big[1 + \frac{1}{n-1} \sum_{w \in \mathcal{N}_v} (x_w(t) - x_w(t-1))\Big]. \quad (3)$$

In the above, the parameters α_v, γ_v and τ_v are non-negative constants that satisfy $\alpha_v + \gamma_v + \tau_v = 1$ for all $v \in \mathcal{V}$. As a result, each payoff $\pi_v(0)$ and $\pi_v(1)$ is a convex combination of three summands. The first term encapsulates a social coordination mechanism, which is typical of game-theoretic ABMs for social diffusion [5], [20]: individual v's payoff increases by adopting the same strategy as their neighbours. The other two terms capture important social-psychology mechanisms, and their incorporation into the payoff function of a game-theoretic ABM for social diffusion was first propose in [1]. Specifically, the second one captures an inertia mechanism [31], incentivising the individual to stick with their current choice. The third term encapsulates a trend-seeking mechanism [32]: individuals increase their payoff by choosing the strategy which has increased in prevalence across the entire population from the previous time-step $t-1$ to the current time-step t, captured by the term $\hat{x}_v(t)$ in Eq. (3). A flow chart representing the operating mechanism of the model is illustrated in Fig. 1.

The ABM presented in this paper first appeared in [1], where it was demonstrated that, during social diffusion, incorporating all three mechanisms in the payoff function enabled the model to closely match the empirical data at both the individual- and population-level. Ref. [1] showed that the inertia mechanism produced a long time delay before adoption of the alternative took off, while the trend-seeking mechanism ensured an explosive transition from a majority adopting the status quo to the majority adopting the alternative; this long delay and rapid diffusion closely describes the classical 'S-shaped' adoption curve from empirical studies [16], [17]. In addition, Ref. [1] parametrised the model using the empirical data collected, obtaining values for $\beta_v, \alpha_v, \gamma_v$, and τ_v, with the model implemented on an all-to-all network structure. In

this paper, building on that experimentally-grounded ABM, we have introduced a network structure to constrain the interactions between the agents while retaining the parameter values in [1], and we aim to investigate the impact of such a network on the diffusion process.

C. Network Classes

In this work, we explore the impact of the network topology on the social diffusion process. To this aim, we consider four classes of synthetic networks, which are classical within the network science literature [33]. Subsequently, we consider a real-world network from an empirical dataset. Here, we review the four different network classes and describe the process for generating networks in each class.

1) Random d-regular (RR) Networks: A class of networks in which every node is randomly connected to d other nodes, and thus all nodes have degree d, for an integer $d \geq 1$. We generate an RR network using a configuration model. First, we give each node d 'tentacles' and we create a 'tentacle pool'. Then, we pick a pair of 'tentacles' from the pool uniformly at random. If these two 'tentacles' belong to two distinct nodes that are not connected by an edge, an edge is added between the two nodes and the two 'tentacles' are removed from the pool. The network formation process terminates when all 'tentacles' are removed from the 'tentacle pool' [20].

2) Erdős–Rényi (ER) Networks: A class of networks in which every pair of nodes is connected by an (undirected) edge with probability $p \in (0, 1)$, independent of every other pair of nodes. For large-scale networks, the degree distribution of an ER network follows a Poisson distribution, with average $d = (n-1)p$.

3) Barabási–Albert (BA) Networks: A class of networks, generated as follows. Starting from a fully connected network with n_0 nodes termed as hubs, we add the remaining $n - n_0$ nodes to the network one by one, and each newly added node is connected to m existing nodes. In particular, the probability of a new node connecting to an existing node i is proportional to the degree of node i. Large-scale BA networks are good proxies of real-world networks, since they are characterised by the scale-free property, i.e. the degree of the nodes follow a power-law distribution [33], with average degree $d = 2m$. In our simulations, we set the number of hubs at $n_0 = d + 1$.

4) Watts-Strogatz (WS) Networks: A class of networks in which the geodesic distance between any two nodes is typically small relative to the number of nodes in the network (the average geodesic distance grows proportionally to the logarithm of the number of nodes n). Hence, WS networks replicate the so-called small-world characteristic and the presence of clusters, which is observed in many real-world social networks [33]. We generate a WS network by firstly creating a ring lattice network with n nodes in which every node is connected to its d nearest nodes, with $d \geq 2$ an even integer. Then, we rewire each edge with a probability p_{ws} independently. If an edge is rewired, we in fact remove the edge and randomly select one of the two nodes that had been connected by this edge. We then connect this chosen node to one of the other $n - 2$ nodes in the ring, selected uniformly at random. Note that, despite having small geodesic distances between any two nodes, WS networks are characterised by a fairly homogeneous degree distribution, concentrated around the average degree d.

When exploring the impact of the network on social diffusion, we will focus on the effect of average degree, d, and global clustering coefficient c. While the former has been extensively discussed in the above, the latter is defined as

$$c = \frac{\sum_{i,j,k \in \mathcal{V}} a_{ij} a_{jk} a_{ki}}{\sum_{i \in \mathcal{V}} d_i (d_i - 1)}, \tag{4}$$

and captures the fraction of closed triadic interactions in the network. While RR, ER, and BA networks are fully characterised by a single parameter (d, p, and m, respectively) which allows us to set only the average degree[1], the generation of WS networks allows for setting an additional parameter (the re-wiring probability). This parameter can be used to regulate the global clustering coefficient [33]. In fact, to obtain clustering coefficient c, we can set the rewiring probability as

$$p_{ws} = 1 - \sqrt[3]{\frac{4c(d-1)}{3(d-2)}}. \tag{5}$$

D. Centrality Approaches

In the second part of our study, we will examine the possibility to place the committed individuals in the most "important" nodes, in order to accelerate the diffusion process. The notion of importance of a node, however, is not univocal. In fact, different approaches, termed centrality measures, have been proposed to rank nodes by their importance [33]. Our study will compare different centrality approaches to inform our placement of committed individuals. Specifically, the approaches are degree, eigenvector, closeness, betweenness, and Bonacich centrality [33]. Note that because we compare the relative values of centrality between nodes, it is not necessary to perform a normalisation of the values.

1) Degree centrality: In this approach, the centrality of a node $v \in \mathcal{V}$ is equal to its degree d_v, so that the higher the degree of a node, the greater its degree centrality.

2) Eigenvector centrality: In this approach, a node is considered "important" if is connected to many important nodes. Formally, let ϕ_v denote the eigenvector centrality of node $v \in \mathcal{V}$, and $\boldsymbol{\phi} = [\phi_1, \ldots, \phi_n]^\top$ denote the vector of centralities. Then, the eigenvector centrality is given by $\boldsymbol{A}\boldsymbol{\phi} = \lambda_{\max}\boldsymbol{\phi}$. Here, $\lambda_{\max}$ is the eigenvalue of the adjacency matrix $\boldsymbol{A}$ with largest real part. Note that because $\mathcal{G}$ is connected and undirected, $\boldsymbol{A}$ is an irreducible symmetric matrix and thus the Perron-Frobenius Theorem establishes that $\lambda_{\max}$ is real and unique [35].

3) Closeness centrality: This approach evaluates the mean geodesic distance from a given node to all other nodes in a network. Formally, the closeness centrality of node $v \in \mathcal{V}$, is computed as

$$\theta_v = \sum_{j \in \mathcal{V} \setminus \{v\}} \frac{n-1}{\ell_{vj}}, \tag{6}$$

[1]For ER networks, the inherent stochasticity allows only for setting the expected average degree, letting $p = d/(n-1)$ and not each realisation.

where ℓ_{vj} is the geodesic distance between nodes v and j. Note that a node with larger closeness centrality θ_v, has a *smaller* mean geodesic distance to other nodes.

4) Betweenness centrality: This approach measures the extent to which the node stands on the communication paths of other pairs of nodes. Formally, the betweenness centrality of node $v \in \mathcal{V}$ is equal to

$$\zeta_v = \sum_{i,j \in \mathcal{V} \setminus \{v\}} \frac{\delta_{ij}(v)}{\delta_{ij}} \ , \tag{7}$$

where δ_{ij} denotes the total number of shortest paths between nodes i and j, and $\delta_{ij}(v)$ is the number of those paths that pass through node v.

5) Bonacich centrality: This approach aims to take into consideration the two ideas of *reachability* and *power*. On the one hand, an individual is considered more reachable if their neighbours have more connections, since this individual thus has a path to a greater number of other individuals within a give number of hops [36]. On the other hand, an individual is more powerful if their neighbours have fewer connections, because by assuming that influence is uniform, an individual's influence on their neighbour increases as their neighbour's degree decreases. To formalise this idea, the Bonacich centrality $\boldsymbol{\mu} = [\mu_1, \cdots, \mu_n]^\top$ is computed as

$$\boldsymbol{\mu} = \left(\boldsymbol{I} - \frac{\eta}{\lambda_{\max}} \boldsymbol{A} \right)^{-1} \boldsymbol{A} \mathbf{1}_{\boldsymbol{n}} \ , \tag{8}$$

where $\boldsymbol{I}$ is the identity matrix, $\mathbf{1}_{\boldsymbol{n}}$ is the all-1 vector, $\lambda_{\max}$ is the largest eigenvalue of the adjacency matrix $\boldsymbol{A}$, and $\eta \in [-1, 1]$ is a constant termed *attenuation factor*. If the attenuation factor η is positive (negative, respectively), nodes with higher Bonacich centrality are more reachable (powerful, respectively). When $\eta = 0$ and $\eta = 1$, the Bonacich centrality is equal to degree centrality and eigenvector centrality, respectively. The magnitude of the attenuation factor can be thought of as capturing a 'radius' around each node for which reachability or power is computed.

E. General Simulation Setup and Research Questions

We are now in a position to describe how we use the game-theoretic model to study a social diffusion scenario, the general simulation setup, and formalise the research questions to be investigated in this paper. In each of our simulations, there are $n = 1,000$ individuals. At $t = 0$, we set initial conditions so that all individuals choose the status quo (i.e. $x_v(0) = 0$ for all $v \in \mathcal{V}$). Then, at $t \geq 1$, we introduce a set of individuals called the *committed minority*, who always stubbornly select the alternative (strategy 1). When not differently stated, committed minority are introduced in the network at $t = 1$ by choosing nodes uniformly at random. We use $\rho_c \in [0, 1]$ to denote the fraction of the population who are committed minority individuals. As identified experimentally in [1], the rest of the uncommitted population are divided into two distinct classes of individuals (termed explorers and non-explorers) and we use $\rho_e \in [0, 1]$ to denote the fraction of explorers in the *uncommitted* population. Each class of individuals is characterised by a common set of values for the parameters α_v, γ_v and τ_v. Specifically, we set at $\alpha_e = 0.48$, $\gamma_e = 0.10$, and $\tau_e = 0.42$ for explorers; and $\alpha_{ne} = 0.42$, $\gamma_{ne} = 0.42$, $\tau_{ne} = 0.16$, for non-explorers. The rationality of all uncommitted individuals is set at $\beta_v = 7.8$. These agent parameter values were identified in [1] from experimental data. Even though these parameters were obtained from experiments in all-to-all networks, we believe it is unlikely that the parameters between all-to-all networks and general networks would deviate by orders of magnitude. Therefore, we decide to use the parameters from [1] in this study, varying the parameter ρ_e to check robustness of our findings, while obtaining empirically-informed parameters for specific networks is a focus for future research.

Given the probabilistic nature of the model in Eq. (1), where each uncommitted agent has a positive probability to play strategy 1 at each time t, full diffusion eventually occurs almost surely. However, such an event may occur only after an extremely long time, and thus it may be never observed in practice. Hence, the key question is to examine, given a network $\mathcal{G}$ and the model parameters, the time for diffusion to occur, termed *diffusion time*. Namely, we wish to identify whether diffusion will occur within a reasonable time-window or take arbitrarily long to occur. In the latter scenario, we say that the model predicts that diffusion *will not occur* in the real-world, because such a large diffusion time would suggest the committed minority die out or give up, a new alternative emerges, or some other exogenous change occurs rendering the model scenario irrelevant. Hence, we consider a fixed simulation time-window of $T_{\max} = 20,000$ time-steps, and we say that diffusion occurs if at least 90% of the uncommitted individuals choose the alternative at the same time-step, within the simulation time-window. The diffusion time is defined as the earliest time-step at which diffusion occurs, defined by

$$T^* = \inf \left\{ 0 \leq t \leq T_{\max} : \frac{1}{n(1-\rho_c)} \sum_{v \in \mathcal{V} \setminus \mathcal{C}} x_v(t) \geq 0.9 \right\}, \tag{9}$$

where $\mathcal{C}$ denotes the set of committed individuals. We stop the simulation if either full diffusion is observed or we reach $T_{\max}$ time-steps. We say that a simulation run is a 'successfully diffused simulation run' if $T^* < +\infty$.

Due to the stochastic nature of the model, we employ a Monte Carlo approach to estimate the probability that a successful diffusion occurs and the corresponding expected diffusion time. Specifically, and in order to obtain insightful observation while minimising the effect of noise, we run 100 independent simulations for each particular set of simulation parameters. The two outputs (i.e. the two criteria of diffusion speed) of the Monte Carlo simulations are i) the percentage of successfully diffused simulation runs, denoted by f_d, which is an *estimate of the diffusion probability*, and ii) the arithmetic mean of the diffusion time of the successfully diffused simulation runs, denoted by $\overline{T^*}$. We point out that $\overline{T^*}$ is computed only over the successfully diffused simulation runs, i.e. over those runs with $T^* < \infty$. Hence, $\overline{T^*}$ is not defined if $f_d = 0$.

We use the two criteria defined above, viz. f_d and $\overline{T^*}$, to characterise *diffusion speed*. Moving from fully connected networks studied in [1] to general connected networks, we wish to study how a variety of factors such as the network structure, and the number of committed minority and their

placement, influence social diffusion and in particular diffusion speed. The research questions are now formally detailed.

Research Question 1: The first research question is to determine how the diffusion speed is impacted by different network topology structures, i.e. the four different network classes introduced in Section II-C, and network characteristics including average degree and global clustering coefficient.

Research Question 2: The second question concerns where one should locate committed minority on a network to accelerate the diffusion speed. The different centrality approaches described in Section II-D will be used to find the most appropriate positions for the committed minority.

Research Question 3: The third question explores whether introducing committed minority gradually can accelerate the diffusion process. To be more precise, most studies into social diffusion assume that all committed individuals are introduced at the start. However, people's sensitivity to trends [32] opens up a question as to whether we can gradually introduce committed individuals over a certain number of time-steps to generate a trend and exploit the trend-seeking mechanism to accelerate social diffusion.

III. Question 1: Impact of Network Topology

A. Simulation Setup

We employ Monte Carlo simulations to study the diffusion model on the four classes of networks presented in Section II-C and on fully connected networks, to investigate Research Question 1. To enable a systematic comparison between the four network classes (which can have significantly different topological characteristics), we compare simulation outcomes for RR, ER, BA and WS networks with the same average degree, d. Namely, we run a series of simulations for the four network classes with $d \in \{4, 8, 12, 16, 20, 100\}$. To ensure the reliability of the conclusion of our study, we also run simulations on an all-to-all network, which serves as a baseline scenario in which the network topology has no impact on social diffusion. The global clustering coefficient is set at $c = 0.25$ for WS networks by suitably setting the re-wiring probability using Eq. (5), and we vary the fraction of explorers in $\rho_e \in \{0.25, 0.5\}$. In all the simulations, committed minority is introduced in a fraction ρ_c of nodes, chosen uniformly at random.

B. Diffusion Probability

First, we compare the estimated diffusion probability f_d on the four classes of networks and on fully connected network as a function of the committed minority fraction ρ_c. The results for RR networks are shown in Fig. 2(a); the results for the other networks, which are qualitatively similar to RR networks, can be found in the Supplementary Material (Figs. S1-S3).

From Fig. 2(a), we observe that the curves are all qualitatively similar, whereby there exists a threshold value of committed minority fraction ρ_c^* such that below the threshold, almost all simulations fail to diffuse, while above the threshold, f_d increases rapidly as ρ_c increases, to reach $f_d = 100\%$. Notice that the value of the threshold ρ_c^* increases as average degree increases; this is also observed in ER, WS and BA network classes (see Supplementary Material, Figs. S1-S3), suggesting that it is easier to achieve social diffusion in sparser networks. However, the effect of the average degree on ρ_c^* diminishes asymptotically as d grows large.

Providing rigorous analytical support for this observation is nontrivial due to the stochastic nature of the model and the complexity of the network topology, and is thus beyond the scope of this paper. Nonetheless, we offer here some quantitative intuition by examining the strategy selection probability for an arbitrary individual i, which is ultimately determined by which one of the two payoffs in Eq. (2) is larger. Specifically, we observe that the first term of Eq. (2a) is larger than the first of Eq. (2b) if and only if the majority of the neighbours of i adopts the innovation. If the d_i neighbours of i are sampled randomly, then the probability of observing a majority of innovators even though the innovators are in the minority rapidly decreases as d_i increases, due to the central limit theorem. As a consequence, as the average degree increases, the probability that an arbitrary agent switches to the alternative when the status quo is still adopted by the majority decreases, thereby reducing the chances to observe social diffusion.

Figure 2(b) confirms this intuitive observation, showing that the committed minority threshold ρ_c^* on all four classes of networks are smaller than the threshold for a fully connected network. Moreover, this figure also allows us to compare the effect of different network topology classes. In particular, we observe that the WS network threshold value ρ_c^* is significantly lower than the ρ_c^* of the other three network classes, which are instead comparable (this is consistent across different values of average degree d). Finally, we observe that, while the threshold for the other networks is extremely sharp, BA networks have a smother transition from 0% to 100% of diffusion. We conjecture that this smoother transition may be due to the high heterogeneity in the BA network, which amplifies the effect of stochasticity.

C. Diffusion Time

Figures 2(c) and 2(d) show the diffusion time as a function of the committed minority fraction ρ_c for RR networks with different average degree and for the four different network classes with $d = 4$, respectively[2]. We observe that there are similarities and differences between the patterns of the diffusion probability (Figs. 2(a)–2(b)) and of the diffusion time (Figs. 2(c)–2(d)). Specifically, here there is also a threshold value of ρ_c above which $\overline{T^*}$ decreases rapidly. This threshold value mostly coincides with ρ_c^* from the previous subsection, and the same observations made in the above concerning the impact of the average degree and of the network structure still hold. However, we observe that the diffusion time is more affected by the stochasticity of the process and the transition between slow diffusion to fast diffusion is less sharp. The error bars in Fig. 2(c) illustrating the 95% confidence interval

[2]The curves for WS, ER, BA, and fully connected networks are similar to the ones for RR networks in Fig. 2(c) and are reported in the Supplementary Material, Figs. S6-S8.

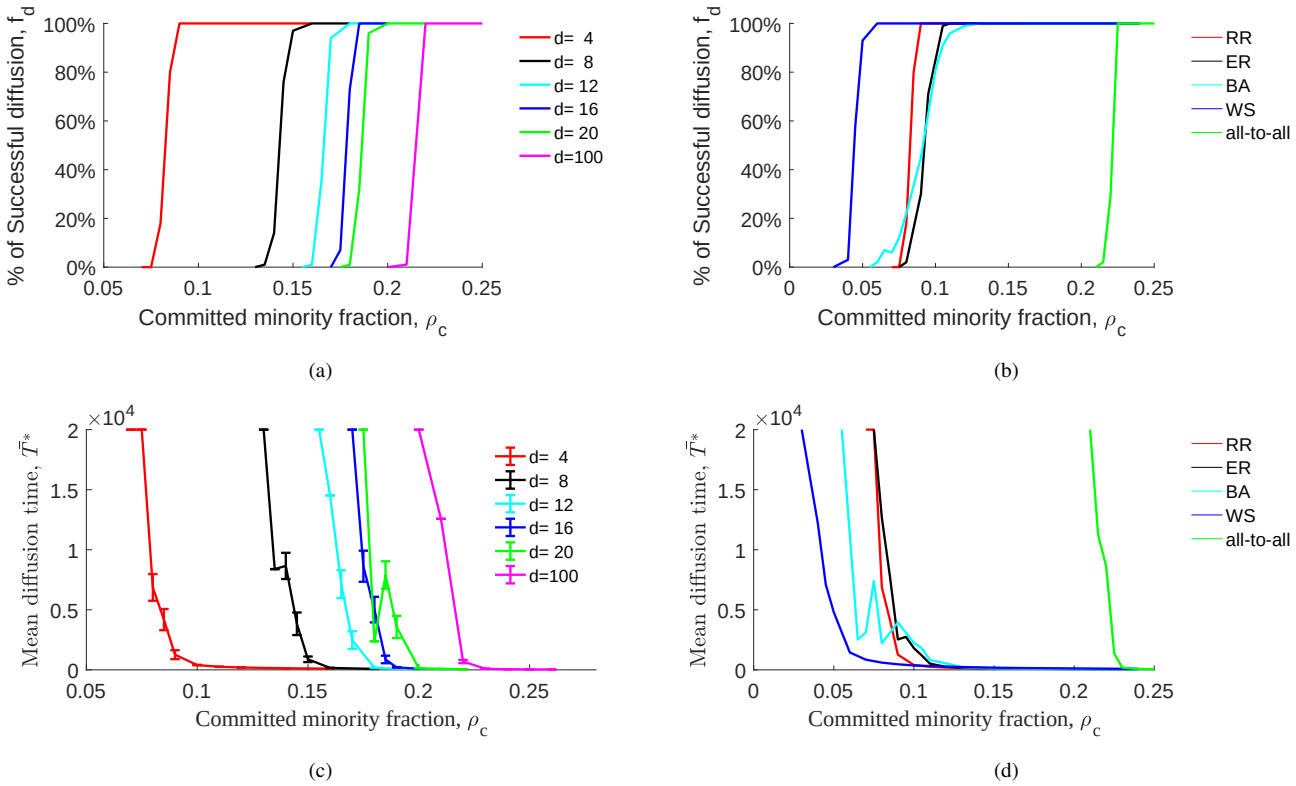

Fig. 2. Simulation results for Research Question 1. In (a,b), we report the estimated diffusion probability on (a) RR networks with different average degree d, and (b) different networks with $d = 4$, and fully connected (all-to-all) network. In (c,d), we report the mean diffusion time and corresponding 95% confidence interval on (c) RR networks with different average degree d, and (d) on different networks with $d = 4$. Common parameters are $\rho_e = 0.5$ and $n = 1,000$.

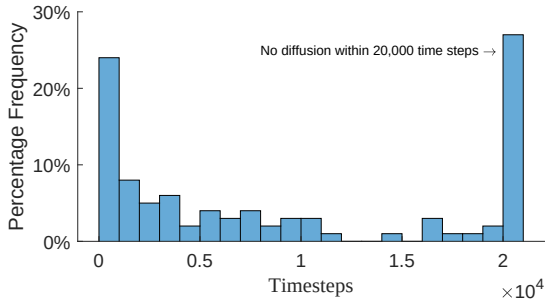

Fig. 3. Distribution of diffusion time T^* for RR networks ($d = 16$, $\rho_e = 0.5$, and $\rho_c = 0.18$). The mean diffusion time is $\overline{T^*} = 5,016.5$.

of T^* confirms this finding, showing how the distribution of the diffusion time gets broader as ρ_c approaches the threshold ρ_c^*. This increased stochasticity is especially visible for BA networks (cyan curve in Fig. 2(d)), also explaining the lower sharpness observed in the transition in the diffusion probability f_d.

To gain more insight into these aspects, we now examine the distribution of diffusion times over the 100 independent simulation runs. By observing the histogram of the diffusion time reported in Fig. 3, we find that distribution patterns on four classes of networks and fully connected network are similar (more figures can be found in the Supplementary Material, Figs. S9-S11). Overall, we observe that the proportion of diffusion times that lie within $2,000 - 18,000$ time-steps is relatively small. In fact, when the system is far from the threshold ρ_c^*, the distribution is unimodal with a peak at one of the two extremes: at $0 - 2,000$ time-steps if $\rho_c \gg \rho_c^*$, or at $> 20,000$ time-steps if $\rho_c \ll \rho_c^*$ (the latter meaning no diffusion has occurred). Close to the threshold, instead the distribution is typically bimodal, with peaks on both extremes. Interestingly, this means that when the committed minority fraction is (slightly) below the threshold, full diffusion can still occur quickly in some simulation runs even though full diffusion does not occur in most simulation runs by $T_{\max}$; this is a consequence of the stochastic nature of the model. However, if diffusion occurs, T^* is typically small.

D. Role of the Clustering Coefficient

As we noted when discussing Fig. 2(b), given any fixed value of d, the value ρ_c^* for WS networks is the smallest among the four classes of networks. This suggests that the specific properties of WS networks may be crucial for favouring social diffusion. In particular, compared with the structure of the other three networks, a key characteristic of WS networks is the higher global clustering coefficients c. Hence, we conduct a further investigation on WS networks by performing an additional campaign of Monte Carlo simulations in which we vary $c \in \{0.1, 0.2, 0.25, 0.4, 0.6\}$, and study the diffusion speed. We fix the average degree and the fraction of explorers at $d = 8$ and $\rho_e = 0.25$, respectively.

The results of our simulations are summarised in Fig. 4. In particular, from Figs. 4(a) and 4(b), we observe that on

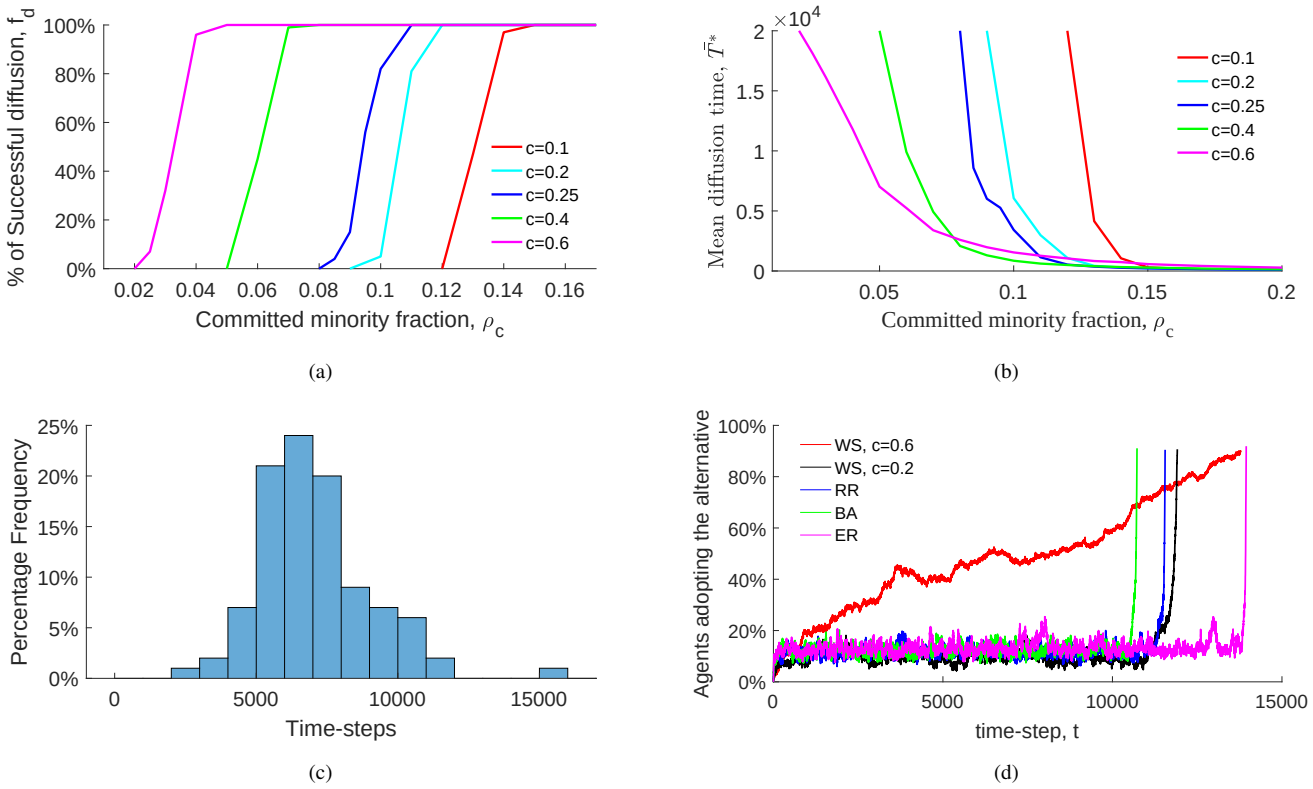

Fig. 4. Additional simulations for Research Question 1. In (a–b), we consider WS networks, and we report (a) the estimated diffusion probability and (b) mean diffusion time for different values of the clustering coefficient c. In (c), we report the diffusion time distribution on the WS Network with $c = 0.6$ and $\rho_c = 0.05$. In (d), we show the fraction of individuals adopting the alternative strategy over time for single representative simulation runs. The committed minority fraction is set to $\rho_c = 0.15$ for RR ER and BA networks; $\rho_c = 0.11$ and 0.04 for WS networks with $c = 0.2$ and $c = 0.6$, respectively (the committed minority fraction is selected differently for the networks, so that it is always close to the threshold ρ_c^*). Common parameters are $\rho_e = 0.25$, $n = 1,000$, and $d = 8$.

WS networks, the larger the global clustering coefficient c, the smaller the threshold value ρ_c^*. A similar behaviour is generally observed also in terms of the mean diffusion time $\overline{T^*}$: when ρ_c is small, we generally observe that $\overline{T^*}$ is smaller if c is larger. However, this relationship becomes insignificant when the committed minority fraction is above the threshold for all networks. In fact, we can see that when $\rho_c > 0.15$, there is virtually no difference in the mean diffusion time for $c \in \{0.2, 0.25, 0.4\}$: fast diffusion occurs in all the scenarios. Interesting is the behaviour for extremely clustered WS networks (magenta curve). For such networks, the threshold ρ_c^* is extremely small. However, the mean diffusion time remains generally quite large even above the threshold. Briefly, the intuition is that in highly clustered networks it is easier to achieve social diffusion, but harder to achieve it quickly. Next, we provide further evidence to support such a claim.

As can be seen by comparing Fig. 4(c) with Fig. 3, the distribution of T^* on the WS networks with large global clustering coefficient are very different from those on RR, ER and BA networks and also different from WS networks with small-to-medium global clustering coefficient (recall that we set $c = 0.25$ in Section III-B). Specifically, Fig. 4(c) shows that T^* is approximately normally distributed with a mean of $\overline{T^*} \in (6000, 7000)$.

Finally, Fig. 4(d) illustrates some representative simulation runs of the diffusion process over time for the different network topologies, with parameters chosen so that the system is in proximity of the threshold ρ_c^*. We can see that the diffusion patterns on RR, ER, BA, and WS networks with $c = 0.2$ are extremely similar. Namely, after a long time period in which the status quo is the overwhelming majority strategy, there is a tipping point and the fraction of the individuals who adopt the alternative strategy increases explosively; full diffusion occurs very shortly after the tipping point. A similar diffusion pattern, where there is a delay followed by explosive diffusion, is observed by Ye *et al.* in experimental data and, numerically, on fully connected networks [1]. However, the diffusion on WS networks with a large global clustering coefficient of $c = 0.6$ has a different pattern. There is no explosive diffusion and the number of alternative strategy adopters increases at a modest (mostly linear) rate. Video animations of the diffusion process are available (see Supplementary Material) and they provide a visual representation of Fig. 4(d).

Based on all of these observations, we comment on the effect of increasing global clustering coefficient on WS networks. Greater clustering ensures that diffusion is more likely to occur. However, the downside is that if full diffusion does occur, the diffusion can be significantly slower, although this effect is more pronounced when there are fewer committed minority. We provide an intuitive argument to justify our observation. On highly clustered WS networks, the alternative quickly diffuses within some clusters, but the spread between clusters takes a long time due to the scarcity of edges between clusters. These observations are consistent with findings from

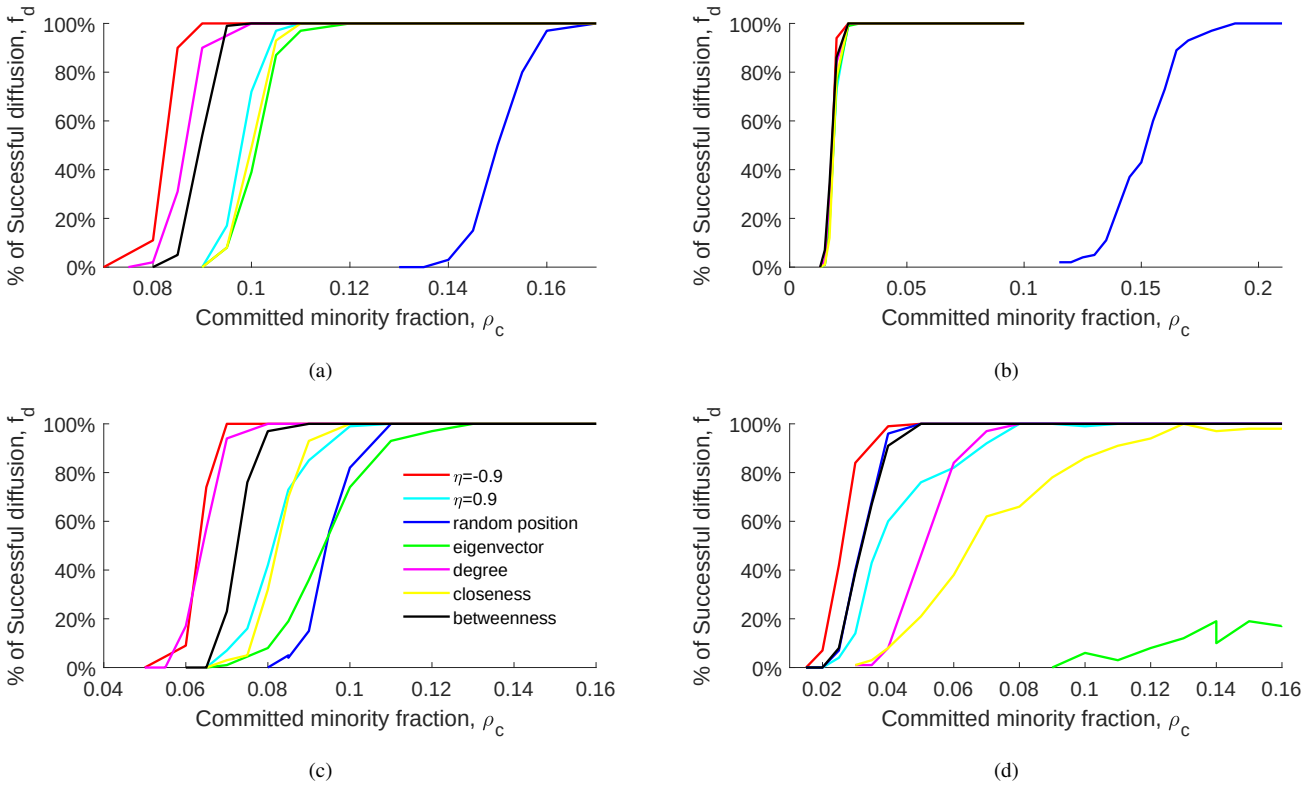

Fig. 5. Simulation results for Research Question 2. Estimated diffusion probability as function of the committed minority fraction for different centrality-based ranking on (a) ER networks, (b) BA networks, (c) WS networks with $c = 0.25$, and (d) WS networks with $c = 0.6$.

other diffusion models, whereby clustering can promote diffusion but the weakness of long-ties between clusters can hinder it [20], [28].

IV. Question 2: Centrality-Based Placement

A. Simulation Setup

Here, we investigate Research Question 2 by comparing different centrality-based approaches to determine the most influential nodes in the network. Specifically, we consider the five centrality measures described in Section II-D, that is, degree, eigenvector, closeness, betweenness, and Bonacich centrality, and we use them to rank the nodes of the network. Then, for each ranking, committed minority are introduced at the nodes with the highest centrality value. Monte Carlo simulation results are compared to the baseline results obtained in the analysis of Research Question 1 in Section III, in which committed minority are introduced uniformly at random. We refer to such a baseline scenario as the *random position approach*. In all simulations, we consider networks with average degree $d = 8$ and set the fraction of explorers to be $\rho_e = 0.25$. Simulations are conducted on the different network structures analysed in Research Question 1, i.e. RR, ER, BA, and two instances of WS networks with $c = 0.25$ and $c = 0.6$.

B. Effectiveness of Centrality-Based Approaches

We start by comparing six different centrality-based rankings. Namely, we consider degree, eigenvector, degree closeness, betweenness, and two different implementations of Bonacich centrality, one with a positive attenuation factor ($\eta = 0.9$) and one with a negative attenuation factor ($\eta = -0.9$); see Section II-D for more details.

The results of our numerical simulations are illustrated in Fig. 5, which reports the estimated diffusion probability f_d, for ER, BA and the two instances of WS networks[3], as a function of the committed minority fraction ρ_c. While the outputs of our simulations seem to change across different network structures, we find several common traits that lead us to make some general observations on centrality-based placement strategies.

First, in most network structures, we observe that where the committed minority is located has indeed a strong impact on the emergent behaviour of the system. In fact, for all networks except the RR network, we observe a significant shift in the threshold ρ_c^*. In general, introducing the committed minority in highly central nodes often seems to be highly effective in favouring social diffusion. It is worth noticing that the only exception to this pattern is recorded for the RR network. In this case, the negligible impact of centrality-based placement is not surprising, since the high regularity of the topology means that most centrality measures to be either equal or differ only slight between all the nodes (e.g. degree centrality); this suggests that all the nodes have a similar influence on the dynamics. However, this is not the case of most real-world networks that, as we shall see in Section VI, do not have such

[3]Results on RR networks are less interesting and reported in the Supplementary Material, Fig. S12.

a regular structure [33], [34].

Second, for the network structures for which the positioning of committed minority impacts the outcome, the extent of such an impact strongly depends on the network topology. In fact, while for ER and WS networks we register moderate shifts in the threshold ρ_c^* with respect to the random position approach (blue curve), such impact seems to be exacerbated by the scale-free structure of the BA network, where using centrality-based approaches seems to yield a ten-fold decrease in the committed minority fraction needed to guarantee social diffusion.

Third, while centrality-based placement approaches seem to be effective in reducing the committed minority fraction needed to guarantee social diffusion, we should observe that, since different centrality measures provide different rankings, the outcomes are often different depending on the measure used. In particular, we register strong differences when considering ER and WS networks (see Figs. 5(c), 5(d), 5(a)) whereas, for BA networks, the centrality measures are extremely highly correlated due to the scale-free structure [33], yielding no significant difference between the results (see Fig. 5(b)).

Finally, we conduct simulations on different population sizes of $n = 2000$ and $n = 500$ (results reported in the Supplementary Material, Figs. S26–S30). By observing those figures, we demonstrate that our findings in Section III and Section IV remain consistent across different population sizes.

C. Impact of Using Different Centrality Approaches

The last observation suggests that not all centrality measures are equally effective in reducing the committed minority fraction needed to unlock social diffusion. This observation calls for further investigation toward understanding which centrality measure is the most effective.

For ER networks, we observe in Fig. 5(a) that all centrality-based approaches seem to decrease the threshold, with the best result attained by the Bonacich centrality with a negative attenuation factor. On mildly clustered WS networks ($c = 0.25$), we record similar results (see Fig. 5(c)). However, in this case, we observe that using the eigenvector centrality (green curve) does not seem to offer any clear advantage with respect to random positioning. Simulations on highly clustered WS networks (reported in Fig. 5(d)) further confirm this observation. Here, the eigenvector approach significantly increases ρ_c^*, which means that using the eigenvector centrality to rank the nodes for placement of committed minority actually *hampers* the diffusion process. Moreover, in such extreme scenario of highly-clustered WS networks, we also observe that some other centrality measures appear to be counterproductive, namely degree and closeness, and Bonacich centrality with a positive attenuation factor. On the contrary, Bonacich centrality with a negative attenuation factor still outperforms the other centrality measures, including random positioning.

To summarise, even though the impact of centrality-based approaches may have strong differences across different network structures, in the above analysis, we have highlighted an important common trait: Bonacich centrality with negative attenuation factor $\eta = -0.9$ seems to be the best approach to effectively decrease the committed minority fraction needed to achieve social diffusion. Finally, additional simulations, reported in Supplementary Material (Figs. S13-S16), suggest that the magnitude of the negative attenuation factor has a minor impact on the outcome of the diffusion process, yielding the conclusion that the best way to insert committed minority in a population is to target nodes with high Bonacich centrality, computed with any negative attenuation factor.

It is worth noticing that, while Bonacich centrality with negative attenuation factors is always optimal, regardless of the magnitude of the attenuation factor chosen, using positive attenuation factors is less beneficial and, sometimes even hinders social diffusion. Such an observation has a twofold implication. First, 'powerful' nodes are more important than 'reachable' nodes in the social diffusion process (see Section II-D on how attenuation factor relates to 'powerful' and 'reachable' nodes). Second, provided the attenuation factor is negative, the magnitude has an insignificant effect on the diffusion speed (recall that the magnitude captures how far-away nodes impact the reachability or power of a node). Finally, we remark that compared with 'reachable' nodes, 'powerful' nodes are connected to a larger number of nodes with lower degree. Our findings in Section III indicate that networks with lower average degree favour diffusion, and this is entirely consistent with our novel observation that placing committed minority at 'powerful' nodes can enhance social diffusion. Intuitively, nodes with lower average degree are more 'isolated', and perhaps more vulnerable to influence from committed minority. These observations are consistent with empirical studies done in different areas of research. For instance, it has been observed that isolated people are more likely to be victims of financial fraud [37], and under certain circumstances more likely to become politically radicalised [38].

V. Question 3: Effect of Timing

A. Simulation Setup

Now that we have established that the positioning of the committed minority can strongly influence social diffusion, we now study the effect of timing. Specifically, we investigate whether gradually introducing committed minority affects the diffusion speed. Hence, we split the committed minority into t_g groups, and we introduce one group every t_p time steps. Formally, the number of committed individuals present in the population at time step t (denoted by $n_c(t)$) is equal to

$$n_c(t) = \begin{cases} \frac{n\rho_c}{t_g}\lceil \frac{t}{t_p} \rceil, & if\ 1 \leq t \leq t_g t_p \\ n\rho_c, & if\ t > t_g t_p \end{cases}, \tag{10}$$

Simulations are conducted on different classes of networks (RR, ER, BA, WS with $c = 0.25$ and $c = 0.6$) with average degree $d = 8$. We consider two distinct scenarios. In the first scenario, we set $t_p = 1$ and we vary $t_g \in \{1, 5, 15\}$. In other words, we gradually increase the number of committed individuals within the first t_g time-steps. In the second scenario, we fix $t_g = 5$, and we consider $t_p \in \{5, 20, 100\}$. That is, we split the committed individuals into 5 groups and introduce one group every t_p time-steps. In all simulations, we introduce committed minority in nodes starting with the highest

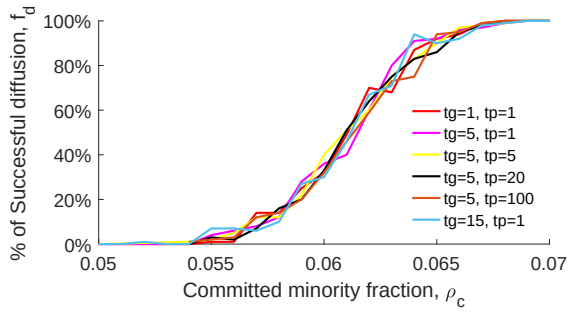

Fig. 6. Simulation results for Research Question 3, illustrating the estimated diffusion probability in the different scenarios.

Bonacich centrality with the attenuation factor $\eta = -0.9$. The fraction of explorers is set at $\rho_e = 0.5$.

B. Result

Figure 6 reports the results of our Monte Carlo simulations for WS networks (results for RR, ER and BA networks are similar and can be found in the Supplementary Material (Figs. S17–S20)[4]). The plots show that the advantages in implementing a gradual introduction of the committed minority with respect to the baseline scenario (red curve) are (if any) very marginal.

To explain such results, we provide the following intuitive analysis. With respect to the scenario in which committed individuals are introduced at $t = 1$, a gradual introduction of the committed minority can enforce the third term in Eq. (2a) (the one associated with sensitivity to trends) to be larger than the one in Eq. (2b) in the time-steps that follow the introduction of committed minority. However, the magnitude of that term is small, since the committed minority is diluted. Moreover, the first term (related to the coordinating mechanism) may decrease too, until the entire committed minority is introduced, weakening its potential impact on social diffusion. Furthermore, we observe that the experimentally obtained payoff coefficients [1] indicated that, regardless of the individual being an explorer or non-explorer, $\alpha_v > \tau_v$, meaning that all things being equal, the coordination term carries a greater weighting for the strategy selection compared to the trend-seeking term. Hence, naive implementations of timely introduction of committed minority might fail in facilitating social diffusion, suggesting that more sophisticated intervention policies should be explored.

VI. Case Studies

In the previous sections, we have investigated the three research questions on different classes of synthetic networks, obtaining some important observations on the impact of key features of the network topology (e.g.sparseness, clustering, scale-free structure) on social diffusion, and on how to design the introduction of committed minority, targeting nodes with high Bonacich centrality. We will conclude the paper by verifying our results on two case studies, in which we use two real-world social network structure, from [34] and [39].

In those two case studies, we perform two sets of simulations, investigating Research Questions 2 and 3, respectively. First, we use the five different centrality approaches tested on the synthetic networks (Section IV) to evaluate the effectiveness of introducing the committed minority in the most central nodes. We compare our results with the scenario in which committed minority are placed at the random positions. In these simulations, the fraction of explorers is set to $\rho_e = 0.25$. Second, we perform the same simulations done in Section V, toward assessing the effectiveness of introducing the committed minority in a gradual fashion. In such scenario, we introduce the committed minority in nodes with the highest Bonacich centrality with attenuation factor $\eta = -0.9$, which is the most effective strategy according to our numerical findings, and we set the fraction of explorers to $\rho_e = 0.5$.

A. Case 1: Coauthorship network

1) Network Structure: We consider a coauthorship network between scientists who have published papers on topics related to 'network structure', discussed in [34]. The dataset is available at [40]. The nodes represent 379 scientists belonging to the largest connected component of the examined dataset; an edge between two nodes means that the two nodes (scientists) have at least one coauthored publication. The network is illustrated in Fig. 7(a), where the diameter of each node is proportional to its Bonacich centrality with the attenuation factor $\eta = -0.9$; the eight most central nodes are in red.

Before presenting the results of our Monte Carlo simulations, we would like to point out some relevant properties of the coauthorship network (more details can be found in [34]). The network has average degree $d = 4.82$ and global clustering coefficient $c = 0.74$. This means that the network exhibits sparsity and high clustering, which is consistent with key characteristics of WS networks. However, the coauthorship network is also scale-free. In fact, the degree distribution of the coauthorship network follows a power-law distribution, which is similar to BA networks. Therefore, the coauthorship network holds characteristics of both WS networks and BA networks, and we expect to observe a behaviour similar to those observed in synthetic networks with these properties.

2) Results: Figure 7(b) illustrates the results of the first set of simulations. Our findings on the coauthorship network are consistent with our conclusions from the analysis of the synthetic networks in Section IV. In fact, we find that centrality-based placement of committed minority has a strong impact on the social diffusion process. However, whether this impact favours or hinders social diffusion depends on the centrality measure used to rank the nodes. In particular, Bonacich centrality with a negative attenuation factor is superior to all other methods, while closeness and eigenvector approach increase the threshold ρ_c^*, similar to what was observed in highly clustered WS networks (see Fig. 5(d)). Moreover, we also find that betweeness and degree centrality are also good ranking approaches, as they decrease the threshold ρ_c^*, as observed for BA networks in Fig. 5(b).

[4]Additionally, we test the scenario in which the committed minority are introduced at random nodes, obtaining similar results (see Supplementary Material, Figs. S21–S25).

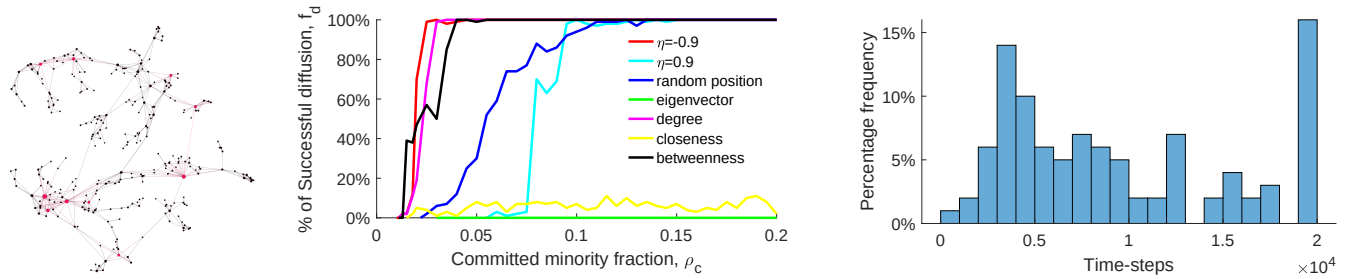

(a) (b) (c)

Fig. 7. Simulation results of the coauthorship network case study in Section VI-A. In (a), we illustrate the network structure. In (b), we report the estimated diffusion probability for different centrality-based rankings. In (c), we report the distribution of diffusion time, for $\rho_c = 0.065$ and $\rho_e = 0.25$; the committed individuals are placed at random position.

In terms of the distribution of diffusion time over 100 independent runs, by observing Fig. 7(c), we find that the distribution is wide. This is a combination of the behaviour of BA networks in which the distribution peaks at the extremes (see Fig. 3) and highly clustered WS networks in which the distribution peaks in the middle (see Fig. 4(c)).

The second set of simulations (results reported in the Supplementary Material, Fig. S31), depict a scenario similar to the one discussed in Section V, where a naive gradual introduction of committed minority seems to have a marginal impact on social diffusion.

B. Case 2: Norwegian boards of directors network

1) Network Structure: In our second case study, we analyse a dataset that portrays the boards of directors of 384 Norwegian public limited companies from September 2010 to August 2011. The network consists of 1,095 nodes, representing individual directors, and an edge between two nodes (directors) indicates that they have served together on the same board at least once. The network is illustrated in Fig. 8(a), where the diameter of each node is proportional to its Bonacich centrality with the attenuation factor $\eta = -0.9$; the ten most central nodes are in red. The average degree of the network is $d = 7.08$, with a power-law distribution, resembling the degree distribution observed in BA networks. Moreover, the network has a large global clustering coefficient of $c = 0.84$, consistent with the characteristic of WS networks. Hence, we can conclude that the Norwegian boards of directors network shares similarities with BA networks and highly-clustered WS networks. As a result, we expect to observe a behaviour similar to what we observed in synthetic BA networks and highly-clustered WS networks.

2) Results: The result of the first set of simulations is as shown in Fig. 8(b). Notably, our observations on the Norwegian boards of directors network closely resemble those made on the coauthorship network. Specifically, we find that centrality-based placement of committed minority has a significant impact on the social diffusion process. In particular, Bonacich centrality with the attenuation factor $\eta = -0.9$ yields the highest promotion of social diffusion, while closeness and eigenvector considerably impede the diffusion process, mirroring observations in highly clustered WS networks. Furthermore, we also find that betweeness and degree centrality favour the diffusion, which is coincident with our observations on BA networks in Fig. 5(b).

The distribution of diffusion time, obtained from 100 independent runs, is given in Fig. 8(c). Similar to the coauthorship network, we observe a wide distribution, as a combination of patterns observed in BA networks (in which the distribution reaches its highest values at the extremes, cf. Fig. 3), and in highly clustered WS networks (in which the distribution tends to peak in the middle, as illustrated in cf. Fig. 4(c)).

In the second set of simulations (in the Supplementary Material, Fig. S32), our findings confirm the conclusions of Section V: a naive gradual introduction of committed minority individuals appears to have a minimal impact on social diffusion.

VII. Discussion and Conclusion

In this work, we studied the influence of network topology structure, the placement of committed minority, and the timing of introducing the committed minority on social diffusion processes. We found that sparser networks tend to accelerate the diffusion process, while Watts–Strogatz networks, especially highly-clustered ones, performed better than other network classes. Concerning how to position the committed minority, we found that using Bonacich centrality with a negative attenuation factor to find the most influential nodes is the best approach. Meanwhile, introducing the committed minority over time in a naive fashion has limited effect.

These findings extend the literature on mathematical modelling of social diffusion by providing novel insights, grounded on an experimentally-validated model [1], to support existing empirical and theoretical studies. In particular, the beneficial effect of network sparsity on social diffusion is consistent with similar observations from other mathematical models [20], [30]. The observation on the key role of clustering in promoting diffusion echoes well-known sociological theories [28] and experimental studies [41], as well as more recent empirical studies on diffusion of COVID-19 [42].

In our second research question, we investigated how to determine the most influential nodes in the network. This problem has been extensively studied in the literature, through many empirical and theoretical studies. Virtually all studies conclude that the position of a node in a network has a strong

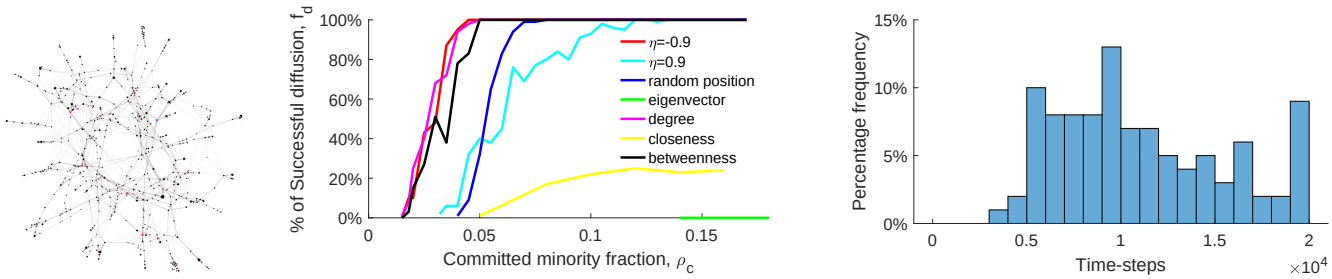

(a) (b) (c)

Fig. 8. Simulation results of the Norwegian boards of directors network case study in Section VI-B. In (a), we illustrate the network structure. In (b), we report the estimated diffusion probability for different centrality-based rankings. In (c), we report the distribution of diffusion time, for $\rho_c = 0.065$ and $\rho_e = 0.25$; the committed individuals are placed at random position.

impact on its influence [22], [43]. However, the centrality measure that should be used to determine the most influential nodes depends on the characteristics of the dynamics considered, e.g. eigenvector centrality for epidemic spreading [44] or betweenness centrality for information diffusion [45]. Our study, performed on an experimentally-validated model for social diffusion, suggests that using Bonacich centrality with a negative attenuation factor is the best approach to introduce the committed minority in this social diffusion scenario. Our findings are consistent with empirical studies on the risk of being victims of financial frauds [37] or political radicalisation [38].

Finally, while there is empirical evidence that people are sensitive to emerging trends [32], in particular during social diffusion [1], little has been investigated on how such sensitivity can be leveraged to design effective interventions to favour social diffusion. Our study contributes to this research direction, suggesting that the design of such policies is a nontrivial problem, since the naive strategies proposed has limited impact.

Although this paper has provided answers to important research questions, several problems remain open. First, we found that the Bonacich centrality is the best approach to positioning committed minority, and it would be useful to compare this against the other optimisation-based methods (such as those arising in influence maximisation problems). Second, the failure of naive strategies introducing committed minority over time suggests that more sophisticated strategy should be designed and tested, potentially leveraging the cluster structure of the network. Third, here we have assumed that individuals have exact information about the ongoing trend. In the future, we plan to consider scenarios in which biased, limited, or just local trend information is available. Fourth, our findings are based on numerical simulations; rigorous mathematical analysis of the model to support these findings is envisaged for future work. Finally, we performed our study using the parameters identified from online experimental data in [1], and varying the proportion of explorers in the population to check robustness. Other experiments should be designed to further verify the robustness of our findings, including identifying parameter values for different network structures (if there is a difference at all) and different social contexts (e.g. the diffusion of conventions vs. technology products, or tight vs. loose cultures).

REFERENCES

[1] M. Ye *et al.*, "Collective patterns of social diffusion are shaped by individual inertia and trend-seeking," *Nat. Commun.*, vol. 12, no. 1, pp. 1–12, 2021.

[2] D. Centola and A. Baronchelli, "The spontaneous emergence of conventions: An experimental study of cultural evolution," *Proc. Natl. Acad. Sci. USA*, vol. 112, no. 7, pp. 1989–1994, 2015.

[3] A. Baronchelli, "The emergence of consensus: a primer," *R. Soc. Open Sci.*, vol. 5, no. 2, p. 172189, 2018.

[4] G. E. Kreindler and H. P. Young, "Rapid innovation diffusion in social networks," *Proc. Natl. Acad. Sci. USA*, vol. 111, no. 3, pp. 10 881–10 888, 2014.

[5] H. Peyton Young, "Innovation Diffusion in Heterogeneous Populations: Contagion, Social Influence, and Social Learning," *Am. Econ. Rev.*, vol. 99, no. 5, pp. 1899–1924, 2009.

[6] ——, "The evolution of conventions," *Econometrica*, pp. 57–84, 1993.

[7] R. A. Winett *et al.*, "Enhancing social diffusion theory as a basis for prevention intervention: A conceptual and strategic framework," *Appl. Prev. Psychol.*, vol. 4, no. 4, pp. 233–245, 1995.

[8] E. Rogers, *Diffusion of Innovations*, 5th ed. New York NY, US: Free Press, 2003.

[9] X. Liu, D. He, and C. Liu, "Information diffusion nonlinear dynamics modeling and evolution analysis in online social network based on emergency events," *IEEE Trans. Comput. Soc. Syst.*, vol. 6, no. 1, pp. 8–19, 2019.

[10] I. M. Otto *et al.*, "Social tipping dynamics for stabilizing earth's climate by 2050," *Proc. Natl. Acad. Sci. USA*, vol. 117, no. 5, pp. 2354–2365, 2020.

[11] L. Zino, M. Ye, and M. Cao, "Facilitating innovation diffusion in social networks using dynamic norms," *PNAS Nexus*, vol. 1, no. 5, p. pgac229, 2022.

[12] D. Centola, J. Becker, D. Brackbill, and A. Baronchelli, "Experimental evidence for tipping points in social convention," *Science*, vol. 360, no. 6393, pp. 1116–1119, 2018.

[13] M. J. Brown and D. Satterthwaite-Phillips, "Economic correlates of footbinding: Implications for the importance of Chinese daughters' labor," *PLOS One*, vol. 13, no. 9, p. e0201337, 2018.

[14] J. Andreoni, N. Nikiforakis, and S. Siegenthaler, "Predicting social tipping and norm change in controlled experiments," *Proc. Natl. Acad. Sci. USA*, vol. 118, no. 16, p. e2014893118, 2021.

[15] T. W. Valente, "Social network thresholds in the diffusion of innovations," *Soc. Netw.*, vol. 18, no. 1, pp. 69–89, 1996.

[16] E. M. Rogers, "Diffusion of preventive innovations," *Addict. Behav.*, vol. 27, no. 6, pp. 989–993, 2002.

[17] F. M. Bass, "A new product growth for model consumer durables," *Manag. Sci.*, vol. 15, no. 5, pp. 215–227, 1969.

[18] L. Zino and M. Cao, "Social Diffusion Dynamics in Cyber–Physical–Human Systems" in *Cyber-Physical-Human Systems: Fundamentals and Applications* (ed. A. M. Annaswamy et al.). John Wiley & Sons, 2023, ch. 3, pp. 43–70.

[19] A. Negahban and P. J. Giabbanelli, "Hybrid agent-based simulation of adoption behavior and social interactions: Alternatives, opportunities, and pitfalls," *IEEE Trans. Comput. Soc. Syst.*, vol. 9, no. 3, pp. 770–780, 2021.

[20] A. Montanari and A. Saberi, "The spread of innovations in social networks," *Proc. Natl. Acad. Sci. USA*, vol. 107, no. 47, pp. 20 196–20 201, 2010.

[21] P. Ramazi, J. Riehl, and M. Cao, "Networks of conforming or non-conforming individuals tend to reach satisfactory decisions," *Proc. Natl. Acad. Sci. USA*, vol. 113, no. 46, pp. 12 985–12 990, 2016.

[22] D. Kempe, J. Kleinberg, and É. Tardos, "Maximizing the spread of influence through a social network," in *Proc. 9th ACM SIGKDD Int. Conf. on Knowledge Discovery and Data Mining*, 2003, pp. 137–146.

[23] F. Fagnani and L. Zino, "Diffusion of Innovation in Large Scale Graphs," *IEEE Trans. Netw. Sci. Eng.*, vol. 4, no. 2, pp. 100–111, 2017.

[24] J. Xie, S. Sreenivasan, G. Korniss, W. Zhang, C. Lim, and B. K. Szymanski, "Social consensus through the influence of committed minorities," *Phys. Rev. E*, vol. 84, no. 1, p. 011130, 2011.

[25] J.-J. Cheng, Y. Liu, B. Shen, and W.-G. Yuan, "An epidemic model of rumor diffusion in online social networks," *Eur. Phys. J. B*, vol. 86, no. 1, pp. 1–7, 2013.

[26] W. Tang, G. Luo, Y. Wu, L. Tian, X. Zheng, and Z. Cai, "A second-order diffusion model for influence maximization in social networks," *IEEE Trans. Comput. Soc. Syst.*, vol. 6, no. 4, pp. 702–714, 2019.

[27] L. Jain, R. Katarya, and S. Sachdeva, "Role of opinion leader for the diffusion of products using epidemic model in online social network," in *Proc. 12th Int. Conf. on Contemporary Computing*, 2019, pp. 1–6.

[28] D. Centola and M. Macy, "Complex Contagions and the Weakness of Long Ties," *Am. J. Sociol.*, vol. 113, no. 3, pp. 702–734, 2007.

[29] M. Kandori, G. J. Mailath, and R. Rob, "Learning, mutation, and long run equilibria in games," *Econometrica*, pp. 29–56, 1993.

[30] G. Ellison, "Learning, local interaction, and coordination," *Econometrica*, pp. 1047–1071, 1993.

[31] W. Samuelson and R. Zeckhauser, "Status Quo Bias in Decision Making," *J. Risk Uncertain.*, vol. 1, no. 1, pp. 7–59, 1988.

[32] G. Sparkman and G. M. Walton, "Dynamic Norms Promote Sustainable Behavior, Even If It Is Counternormative," *Psychol. Sci.*, vol. 28, no. 11, pp. 1663–1674, 2017.

[33] M. Newman, *Networks*, 2nd ed. Oxford, UK: Oxford University Press, 2018.

[34] M. E. J. Newman, "Finding community structure in networks using the eigenvectors of matrices," *Phys. Rev. E*, vol. 74, p. 036104, Sep 2006.

[35] C. D. Godsil and G. Royle, *Algebraic Graph Theory*. New York NY, US: Springer, 2001, vol. 207.

[36] P. Bonacich, "Power and centrality: A family of measures," *Am. J. Sociol.*, vol. 92, no. 5, pp. 1170–1182, 1987.

[37] B. D. James, P. A. Boyle, and D. A. Bennett, "Correlates of susceptibility to scams in older adults without dementia," *J. Elder Abuse Negl.*, vol. 26, no. 2, pp. 107–122, 2014.

[38] C. McCauley and S. Moskalenko, "Toward a Profile of Lone Wolf Terrorists: What Moves an Individual From Radical Opinion to Radical Action," *Terror. Political Violence*, vol. 26, no. 1, pp. 69–85, 2014.

[39] C. Seierstad and T. Opsahl, "For the few not the many? the effects of affirmative action on presence, prominence, and social capital of women directors in Norway," *Scand. J. Manag.*, vol. 27, no. 1, pp. 44–54, 2011.

[40] Gephi, "Datasets," https://github.com/gephi/gephi/wiki/Datasets, 2021, last access: Jun 2023.

[41] D. Centola, "The spread of behavior in an online social network experiment," *Science*, vol. 329, no. 5996, pp. 1194–1197, 2010.

[42] F. Schlosser, B. F. Maier, O. Jack, D. Hinrichs, A. Zachariae, and D. Brockmann, "COVID-19 lockdown induces disease-mitigating structural changes in mobility networks," *Proc. Natl. Acad. Sci. USA*, vol. 117, no. 52, pp. 32 883–32 890, 2020.

[43] J. Sun and J. Tang, "A survey of models and algorithms for social influence analysis," in *Social Network Data Analytics*. Springer US, 2011, pp. 177–214.

[44] P. Van Mieghem, D. Stevanović, F. Kuipers, C. Li, R. van de Bovenkamp, D. Liu, and H. Wang, "Decreasing the spectral radius of a graph by link removals," *Phys. Rev. E*, vol. 84, no. 1, 2011.

[45] L. C. Freeman, "A set of measures of centrality based on betweenness," *Sociometry*, vol. 40, no. 1, p. 35, 1977.

Tianshu Gao received the B.S. degree from Shan Dong University, Jinan, China, in 2010. He received the ME degree from The University of Western Australia, WA, Australia, in 2015. He is currently pursuing a Ph.D. degree with the School of Electrical and Computer Engineering, Curtin University. His current research interests include social diffusion, information diffusion, and network analysis.

Lorenzo Zino (M'21) is an Assistant Professor with the Department of Electronics and Telecommunications at Politecnico di Torino (Turin, Italy), since 2022. He received the BS and MS in Mathematical Engineering from Politecnico di Torino, in 2012 and 2014, respectively, and the PhD in Pure and Applied Mathematics (with honors) from Politecnico di Torino and Università di Torino (joint doctorate program), in 2018. He was a Research Fellow at Politecnico di Torino (2018–19) and the University of Groningen (2019–22), and he visited Lund University (2015), New York University Tandon School of Engineering (2017–18 and 2019), and Curtin University (2023). He is the author of two book chapters and 60+ papers on international journals and conference proceedings. His current research interests include modeling, analysis, and control of dynamics over complex networks, applied probability, and game theory. He is an Associate Editor of the *Journal of Computational Science*, and a member of the Conference Editorial Board for the *IEEE Control Systems Society* and the *European Control Association*.

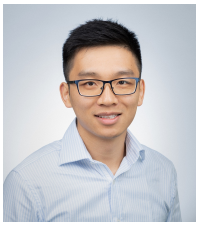

Mengbin Ye (S'13-M'18) was born in Guangzhou, China. He received the B.E. degree (with First Class Honours) in mechanical engineering from the University of Auckland, Auckland, New Zealand in 2013, and the Ph.D. degree in engineering at the Australian National University, Canberra, Australia in 2018. From 2018-2020, he was a post-doctoral researcher with the Faculty of Science and Engineering, University of Groningen, Netherlands. From 2020 - 2021, he was an Optus Fellow at the Optus–Curtin Centre of Excellence in Artificial Intelligence, Curtin University, Perth, Australia. In 2021, he commenced a four year Western Australia Premier's Early to Mid-Career Fellowship, hosted by Curtin University. He was awarded the J.G. Crawford Prize (Interdisciplinary) in 2018, ANU's premier award recognising graduate research excellence. He has also received the 2018 Springer PhD Thesis Prize, and was Highly Commended in the Best Student Paper Award at the 2016 Australian Control Conference. His current research interests include opinion formation and decision making in complex social networks, epidemic modelling and control, and cooperative control of multi-agent systems.